Int. J. Solids Structures Vol. 30, No. 12, pp. 1663–1677, 1993
Printed in Great Britain

0020–7683/93 \$6.00+ .00

BUCKLING OF RECTANGULAR MINDLIN PLATES WITH TAPERED THICKNESS BY THE SPLINE STRIP METHOD

T. MIZUSAWA
Department of Construction and Civil Engineering, Daido Institute of Technology, Hakusuicho-40, Minami-ku, Nagoya 457, Japan

(*Received* 10 *March* 1992; *in revised form* 16 *December* 1992)

Abstract—This paper presents an application of the spline strip method to analyse buckling of rectangular Mindlin plates with linearly tapered thickness in one direction, considering the transverse shear effects and the curvature terms appearing in the expression for loss of potential energy of the applied membrane stresses.

To demonstrate the convergence and accuracy of the present method, several examples are solved, and results are compared with those obtained by an analytical method and by other numerical methods. Stable convergence and excellent accuracy are obtained using the higher order spline strip models.

Buckling load parameters of rectangular thick plates due to uniform in-plane loads with some boundary conditions are analysed by varying plate-aspect ratios, thickness ratios and tapered ratios.

1. INTRODUCTION

Extensive analyses for elastic stability of rectangular plates of both constant thickness and variable thickness on the basis of the classical plate theory have been carried out using the exact method and numerical methods, and a considerable amount of information on the buckling load parameters for different boundary conditions and in-plane loadings is available in the literature (Timoshenko and Gere, 1961; Bulson, 1970; Kobayashi and Sonoda, 1990, 1991). On the other hand, elastic buckling of moderately thick plates based on the Mindlin–Reissner plate theory in which account is taken of the effect of transverse shear deformation, is not so extensive (Leissa, 1982). Srinivas and Rao (1969) presented an exact three-dimensional elastic analysis for the stability of thick simply-supported rectangular plates. Brunelle (1971) analysed the elastic buckling of transversely isotropic Mindlin plates with two parallel edges simply supported and the remaining two edges subjected to a variety of boundary conditions. Brunelle and Robertson (1974) have derived the governing equations of a transversely isotropic, initially stressed Mindlin plate, and solved the thick plate equations for simply-supported rectangular plates in a state of uniform compressive stress plus a uniform bending stress both acting in the same direction. Rao *et al.* (1975) analysed the stability of moderately thick rectangular plates by a triangular finite element. Luo (1982) presented the finite element analysis for the buckling of thin and moderately thick plates by means of a modified complementary energy principle, and showed the simplicity and reliability of the method. Sakiyama and Matsuda (1987) analysed the elastic buckling of rectangular Mindlin plates with mixed boundary conditions using the integral equations combined with the numerical integration technique.

However, these studies based on the finite element method and other numerical methods have ignored the "curvature terms" appearing in the expression for loss of potential energy of the applied membrane stresses. Benson and Hinton (1976) and Hinton (1978) have considered the buckling of Mindlin plates with one pair of opposite edges simply supported using the finite strip method including the presence of the curvature terms or second order strains in the potential energy due to in-plane stresses. Dawe and Roufaeil (1982) analysed the elastic buckling of rectangular Mindlin plates with arbitrary boundary conditions using the Rayleigh–Ritz method and the finite strip method. However, to the author's knowledge, the elastic buckling of rectangular Mindlin plates with varying thickness has not been investigated.

In this paper, spline strip models based on the Mindlin plate theory are used to analyse the buckling of rectangular plates with linearly varying thicknesses, with two parallel edges simply supported and the remaining two edges subjected to a variety of boundary conditions.

To demonstrate the convergence and accuracy of the present method, several examples are solved, and results are compared with those obtained by other numerical methods. Stable convergence and excellent accuracy are obtained using higher order spline strip models. Buckling load parameters of rectangular Mindlin plates with several boundary conditions are analysed by varying aspect ratios, thickness ratios and tapered ratios, and presented in tabular form.

2. SPLINE STRIP METHOD

The solution procedure of the buckling of rectangular Mindlin plates with linearly tapered thickness is based on the spline strip method presented by Mizusawa (1988, 1989), which can be regarded as an alternative form of the thick finite strip method described by Dawe *et al.* (1982).

The plate is idealized by discrete strip elements as shown in Fig. 1.

It is convenient to introduce the non-dimensional coordinate systems

$$\xi = x/a, \quad \eta = y/b, \quad W' = W/b, \tag{1}$$

in which a and b are length and width of the plate, respectively.

The displacement functions of the two rotations and deflection (θ_X, θ_Y, W') in a strip element are expressed by the product of the basic function series in the longitudinal direction and the B-spline functions which are known as piecewise polynomials in the other direction:

$$\theta_X(\xi,\eta) = \sum_{m=1}^{r} \sum_{n=1}^{i_i} A_{nm} N_{n,k}(\eta) \cdot \bar{Y}_m(\xi) = \sum_{m=1}^{r} [\mathrm{N}] \bar{Y}_m(\xi) \{\delta_A\}_m,$$

$$\theta_Y(\xi,\eta) = \sum_{m=1}^{r} \sum_{n=1}^{i_i} B_{nm} N_{n,k}(\eta) \cdot Y_m(\xi) = \sum_{m=1}^{r} [\mathrm{N}] Y_m(\xi) \{\delta_B\}_m,$$

$$W'(\xi,\eta) = \sum_{m=1}^{r} \sum_{n=1}^{i_i} C_{nm} N_{n,k}(\eta) \cdot Y_m(\xi) = \sum_{m=1}^{r} [\mathrm{N}] Y_m(\xi) \{\delta_C\}_m, \tag{2}$$

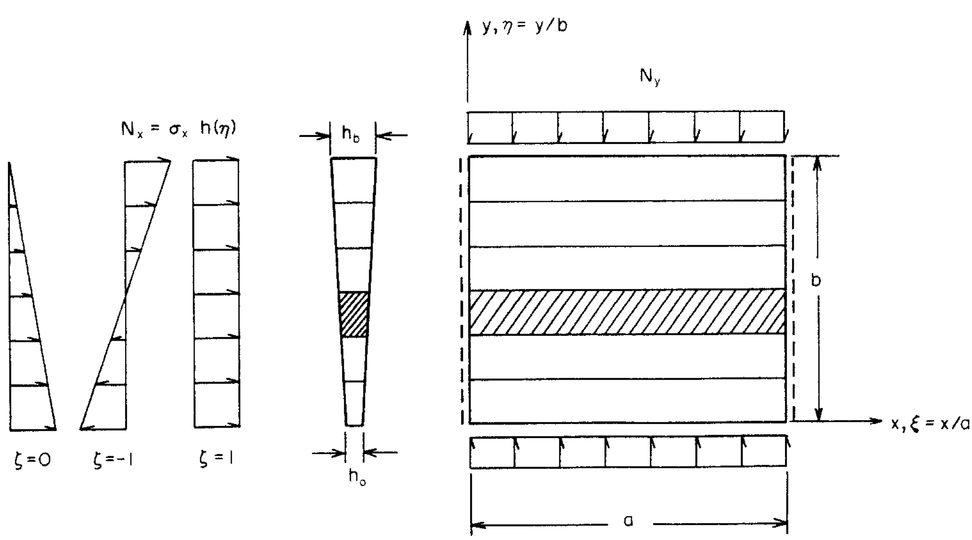

Fig. 1. Rectangular Mindlin plate and coordinate systems.

where

$$[\mathbf{N}] = [N_{1,k}(\eta), N_{2,k}(\eta), \ldots, N_{iy,k}(\eta)] \tag{3}$$

and

$$\{\delta_A\}_m = \{A_{1m}A_{2m}\ldots A_{iym}\}^{\mathrm{T}}, \quad \{\delta_B\}_m = \{B_{1m}B_{2m}\ldots B_{iym}\}^{\mathrm{T}},$$
$$\{\delta_C\}_m = \{C_{1m}C_{2m}\ldots C_{iym}\}^{\mathrm{T}}, \tag{4}$$

in which $i_y = k+M_y-1$, and $\bar{Y}_m(\xi)$ and $Y_m(\xi)$ are the basic functions satisfying the end conditions in the η-direction. $N_{n,k}(\eta)$ is the normalized B-spline function, $k-1$ is the degree of the B-spline function, M_y is the number of strip elements.

Equation (2) can be expressed in matrix form as follows:

$$\{\mathbf{Z}\} = [\mathbf{S}]_m\{\Delta\}_m, \tag{5}$$

where

$$\{\mathbf{Z}\} = \{\theta_X, \theta_Y, W'\}^{\mathrm{T}}, \quad \{\Delta\}_m = \{\{\delta_A\}_m\{\delta_B\}_m\{\delta_C\}_m\}^{\mathrm{T}} \tag{6}$$

and

$$[\mathbf{S}]_m = \sum_{m=1}^{r}\begin{bmatrix}[\mathbf{N}]\bar{Y}_m(\xi) & 0 & 0\\ 0 & [\mathbf{N}]Y_m(\xi) & 0\\ 0 & 0 & [\mathbf{N}]Y_m(\xi)\end{bmatrix}. \tag{7}$$

The $\{\Delta\}_m$ are unknown parameters which can be determined by the minimum total potential energy theorem.

In Mindlin–Reissner plate theory, the generalized strains comprise the curvature changes $(\varepsilon_X, \varepsilon_Y, \varepsilon_{XY})$ and the shear strains $(\gamma_{XZ}, \gamma_{YZ})$ which are defined as follows:

$$\{\varepsilon\}_b = \begin{Bmatrix}(1/a)\,\partial\theta_X/\partial\xi\\ (1/b)\,\partial\theta_Y/\partial\eta\\ (1/b)\,\partial\theta_X/\partial\eta + (1/a)\,\partial\theta_Y/\partial\xi\end{Bmatrix}, \tag{8}$$

$$\{\varepsilon\}_s = \begin{Bmatrix}\theta_X + (b/a)\,\partial W'/\partial\xi\\ \theta_Y + \partial W'/\partial\eta\end{Bmatrix}. \tag{9}$$

Substituting eqns (2) into eqns (8) and (9), and peforming the differentiations, the strain vector $\{\chi\}$ is found to be

$$\{\chi\} = \begin{Bmatrix}\{\varepsilon\}_b\\ \{\varepsilon\}_s\end{Bmatrix} = [\mathbf{T}]\{\mathbf{Z}\} = [\mathbf{T}][\mathbf{S}]_m\{\Delta\}_m = [\mathbf{B}]_m\{\Delta\}_m. \tag{10}$$

The differential matrix operator $[\mathbf{T}]$ and the strain matrix $[\mathbf{B}]_m$ of a strip element are defined as follows:

$$[\mathbf{T}] = \begin{bmatrix}(1/a)\,\partial/\partial\xi & 0 & 0\\ 0 & (1/b)\,\partial/\partial\eta & 0\\ (1/b)\,\partial/\partial\eta & (1/a)\,\partial/\partial\xi & 0\\ 1 & 0 & (1/a)\,\partial/\partial\xi\\ 0 & 1 & (1/b)\,\partial/\partial\eta\end{bmatrix} \tag{11}$$

and

$$[\mathbf{B}]_m = [\mathbf{T}][\mathbf{S}]_m$$

$$= \sum_{m=1}^{r} \begin{bmatrix} (1/a)[\mathbf{N}]\dot{\bar{Y}}_m(\xi) & 0 & 0 \\ 0 & (1/b)[\dot{\mathbf{N}}]Y_m(\xi) & 0 \\ (1/b)[\dot{\mathbf{N}}]\bar{Y}_m(\xi) & (1/a)[\mathbf{N}]\dot{Y}_m(\xi) & 0 \\ [\mathbf{N}]\bar{Y}_m(\xi) & 0 & (b/a)[\mathbf{N}]\dot{Y}_m(\xi) \\ 0 & [\mathbf{N}]Y_m(\xi) & [\dot{\mathbf{N}}]Y_m(\xi) \end{bmatrix}$$

$$= \sum_{m=1}^{r} \begin{bmatrix} [\mathbf{B}_b]_m \\ [\mathbf{B}_s]_m \end{bmatrix}, \tag{12}$$

where $\dot{\bar{Y}}_m(\xi) = \partial \bar{Y}_m(\xi)/\partial\xi$, $\dot{Y}_m(\xi) = \partial Y_m(\xi)/\partial\xi$ and $[\dot{\mathbf{N}}] = \partial[\mathbf{N}]/\partial\eta$.

The thickness of the plate varies in the η-direction in linear fashion as

$$h(\eta) = h_0(\delta\eta + 1), \tag{13}$$

where δ is a tapered ratio expressed by $(h_b - h_0)/h_0$, and h_0 and h_b denote the thickness at the sides of $\eta = 0$ and $\eta = 1$, respectively.

For an isotropic material, the matrices of flexural and shear rigidities are written as

$$[\mathbf{D}]_b = D_0(\delta\eta+1)^3 \begin{bmatrix} 1 & v & 0 \\ v & 1 & 0 \\ 0 & 0 & (1-v)/2 \end{bmatrix}, \tag{14}$$

$$[\mathbf{D}]_s = Eh_0(\delta\eta+1)\kappa/2(1+v) \begin{bmatrix} 1 & 0 \\ 0 & 1 \end{bmatrix}, \tag{15}$$

in which $D_0 = Eh_0^3/12(1-v^2)$. E is Young's modulus, v is Poisson's ratio and $\kappa = \pi^2/12$ is a coefficient to take into account the warping of the section.

The strain energy due to bending and transverse shear deformation, U of the isotropic rectangular Mindlin plate is given in dimensionless coordinate systems (ξ, η, W') as follows:

$$U = (1/2)\int_0^1\int_0^1 [\{\varepsilon\}_b^{\mathrm{T}}[\mathbf{D}]_b\{\varepsilon\}_b + \{\varepsilon\}_s^{\mathrm{T}}[\mathbf{D}]_s\{\varepsilon\}_s]\,\mathrm{d}\xi\,\mathrm{d}\eta$$

$$= (D_0/2)(a/b)\int_0^1\int_0^1 (\delta\eta+1)^3\cdot\{(b/a)^2(\partial\theta_x/\partial\xi)^2 + (\partial\theta_Y/\partial\eta)^2$$

$$+ 2v(b/a)(\partial\theta_X/\partial\xi)(\partial\theta_Y/\partial\eta)$$

$$+ 0.5(1-v)\{(\partial\theta_X/\partial\eta) + (b/a)(\partial\theta_Y/\partial\xi)\}$$

$$+ 6(1-v)\kappa(b/h_0)^2(\delta\eta+1)^{-2}[\{(b/a)(\partial W'/\partial\xi) + \theta_X\}^2$$

$$+ \{(\partial W'/\partial\eta) + \theta_Y\}^2]\}\,\mathrm{d}\xi\,\mathrm{d}\eta, \tag{16}$$

and the strain energy accounting for the second order strain of a tapered plate due to an in-plane compressive load, N_y, and to arbitrarily distributing the compressive load, σ_x, V is also written as

$$V = (ab/2)\int_0^1\int_0^1 [N_y(\partial W'/\partial\eta)^2$$

$$+ (1/12)N_y(h_0/b)^2(\delta\eta+1)^2\{(\partial\theta_x/\partial\eta)^2 + (\partial\theta_y/\partial\eta)^2\}$$

$$+ N_x^0\{\eta(\zeta-1)+1\}(b/a)^2(\delta\eta+1)(\partial W'/\partial\xi)^2$$

$$+(1/12)N_x^0\{\eta(\zeta-1)+1\}(b/a)^2(h_0/b)^2(\delta\eta+1)^3\{\partial\theta_x/\partial\xi)^2$$
$$+(\partial\theta_y/\partial\xi)^2\}]\,\mathrm{d}\xi\,\mathrm{d}\eta, \tag{17}$$

where $N_x^0 = \sigma_x h_0$ and $N_y = \sigma_y h_0(\delta\eta+1)$, ζ is a distributing factor of the compressive stress, σ_x in the η-direction (see Fig. 1) and σ_x and σ_y are compressive stresses.

To deal with arbitrary boundary conditions along two opposite edges ($\eta = 0$ and $\eta = 1$), the method of artificial springs is used. According to this method, three types of springs, α, β and γ, corresponding to deflection and the two rotations, θ_X and θ_Y, respectively, are introduced at each edge of the plate. The energy contribution due to these springs is added to eqn (16) to form the total potential energy for the entire system. The energy contribution, Ub due to these springs is given by

$$Ub = \int_0^1 \{(ab^2W'^2+\beta\theta_X^2+\gamma\theta_Y^2)|_{\eta=0}+(ab^2W'^2+\beta\theta_X^2+\gamma\theta_Y^2)|_{\eta=1}\}\,\mathrm{d}\xi. \tag{18}$$

The functional of the plate, Π, is expressed as follows:

$$\Pi = U+Ub-V. \tag{19}$$

By substituting eqns (2) into eqn (19) and using the principle of minimum potential energy, the coefficients $\{\Delta\}$ are determined as follows:

$$\partial\Pi/\partial\{\Delta\}_s = 0, \tag{20}$$

which may be expressed in matrix form as

$$\sum_{m=1}^{r}\sum_{s=1}^{r}([\mathbf{K}]_{ms}\{\Delta\}_m - n^*[\mathbf{G}]_{ms}\{\Delta\}_m) = 0. \tag{21}$$

Here n^* is a buckling load parameter which may be expressed by $N_y a^2/D_0\pi^2$ or $\sigma_x h_0 b^2/D_0\pi^2$.

The matrices of $[\mathbf{K}]_{ms}$ and $[\mathbf{G}]_{ms}$ are given by

$$[\mathbf{K}]_{ms} = D_0\cdot(a/b)\begin{bmatrix}[K\theta_x\theta_x] & [K\theta_x\theta_y] & [K\theta_x W'] \\ [K\theta_y\theta_x] & [K\theta_y\theta_y] & [K\theta_y W'] \\ [KW'\theta_x] & [KW'\theta_y] & [KW'W']\end{bmatrix}_{ms} \tag{22}$$

and

$$[\mathbf{G}]_{ms} = ab\begin{bmatrix}[G\theta_x\theta_x] & & 0 \\ & [G\theta_y\theta_y] & \\ 0 & & [GW'W']\end{bmatrix}_{ms}. \tag{23}$$

In eqns (22) and (23), the submatrices of $[K_{ij}]$ and $[G_{ij}]$ are defined in the Appendix. The order of these submatrices is expressed by $3r(k+M_y-1)$, where $k-1$ is the degree of the B-spline functions and M_y is the number of strips.

If the two opposite edges are simply supported, the basic functions in eqns (2) can be given by

$$\bar{Y}_m(\xi) = \cos(m\pi\xi), \quad Y_m(\xi) = \sin(m\pi\xi); \quad (m = 1,2,\ldots,r). \tag{24}$$

Their properties of orthogonality result in matrices which have no coupling between the different terms and therefore a term by term analysis involving only small matrices can be carried out. Thus, the solution of the Mindlin plate with the two opposite edges simply supported is obtained by

$$([K_{nq}]_{mm}\{\Delta\}_m - n^*[G_{nq}]_{mm}\{\Delta\}_m) = \{0\}; \quad \begin{array}{l} m = 1,2,\ldots,r, \\ n,q = 1,2,\ldots,i_y. \end{array} \tag{25}$$

A family of strip models can be generated, corresponding to different degrees of B-spline interpolation across a strip. To perform the integrations required in determining $[K_{nq}]$ and $[G_{nq}]$, analytical (full) integration is always used.

3. NUMERICAL EXAMPLES AND DISCUSSIONS

The buckling of isotropic rectangular Mindlin plates with linearly tapered thickness in one direction subjected to in-plane compressive loads is solved to illustrate the convergence and accuracy of the present method. The two opposite edges parallel to the η-direction are simply supported and the other two edges may be arbitrary boundary conditions.

For the definition of the boundary conditions along the edges, the symbolism SS-CF, for example, identifies a rectangular plate with the edges $\xi = 0$, $\xi = 1$, $\eta = 0$, $\eta = 1$ having simply-supported, simply-supported, clamped and free boundary conditions, respectively. Buckling mode shapes are described in the form (i, j) where i and j are the numbers of half waves in the ξ- and η-directions, respectively. The value of the shear factor, κ, is assumed to be $\pi^2/12$.

Table 1 shows the effect of the degrees of B-spline functions, $k-1$ and the numbers of strips, M_y on the buckling load parameter, $n^* = \sigma_x h_0 b^2/(D_0\pi^2)$ of square Mindlin plates with tapered thickness ($\delta = 1.0$) subjected to the uniform compressive load, σ_x. The ratio of b/h_0 varies from 10 to 1000. The number of strips, M_y, of 4, 8 and 12 is used. The degree of B-spline functions, $k-1$, in a strip element degenerates cubic, quartic and quintic interpolation.

Good convergence is obtained with an increase in the number of strips and in the degreee of the B-spline functions. The high-order strip model is shown to be rapidly convergent. In view of this study, we restrict ourselves here to use of the quintic B-spline functions ($k-1 = 5$) in order to obtain more accurate upper bound solutions of rctangular Mindlin plates with tapered thickness in one direction having one pair of opposite edges simply supported.

The comparison study on the buckling load parameter, $n^* = N_y a^2/(D_0\pi^2)$ for thin

Table 1. Convergence study of buckling load parameter, $n^* = \sigma_x h_0 b^2/D_0\pi^2$, for square plates (SS-CC) with linearly varying thickness in the η-direction subjected to the uniform compressive load, σ_x : $b/a = 1.0$, $\nu = 0.3$, $\delta = (h_b - h_0)/h_0 = 1.0$ and $\zeta = 1$

		b/h_0					
		SS-CC			SS-CF		
$k-1$	M_y	1000	100	10	1000	100	10
	4	37.050	17.375	10.945	4.9416	4.2468	3.5713
3	8	17.739	16.274	10.922	4.2809	4.1690	3.5675
	12	16.630	16.213	10.921	4.1970	4.1638	3.5674
	4	17.549	16.320	10.924	4.2377	4.2213	3.5679
4	8	16.363	16.206	10.921	4.1790	4.1637	3.5674
	12	16.298	16.204	10.921	4.1764	4.1617	3.5674
	4	16.442	16.210	10.922	4.1813	4.1656	3.5675
5	8	16.294	16.204	10.921	4.1762	4.1623	3.5674
	12	16.292	16.204	10.921	4.1761	4.1607	3.5674
		(2, 1)	(2, 1)	(2, 1)	(1,1)	(1, 1)	(1, 1)

(i, j) : i, j are the number of half waves in the ξ and η-directions, respectively.

Table 2. Comparison of buckling load parameter, $n^* = N_y a^2/D_0\pi^2$, for thin rectangular plates with tapered thickness in the η-direction subjected to the in-plane compressive load, N_y: $b/h_0 = 1000$, $k-1 = 5$, $M_y = 12$ and $v = 1/3$

Boundary condition	a/b	h_b/h_0 0.0	0.5	1.0	2.0
SS-SS	0.5	6.2500 (6.2500)	11.650 (11.650)	18.438 (18.439)	36.016 (36.017)
	1.0	4.0000 (4.0000)	7.1050 (7.1051)	10.463 (10.464)	18.198 (18.198)
	2.0	4.0000 (4.0000)	5.9528 (5.9527)	7.5478 (7.5471)	10.892 (10.892)
SS-CC	0.5	18.187 (18.187)	33.638 (33.638)	52.472 (52.472)	99.427 (99.404)
	1.0	6.7432 (6.7432)	12.314 (12.313)	18.790 (18.789)	34.157 (34.139)
	2.0	4.8471 (4.8471)	8.1637 (8.1613)	11.298 (11.284)	17.722 (17.844)

( ) is the result calculated by Kobayashi and Sonoda (1991).

rectangular plates ($b/h_0 = 1000$, $v = 1/3$) with tapered thickness in the η-direction subjected to the in-plane compressive load, N_y in the η-direction is shown in Table 2. The strip model with $k-1 = 5$ and $M_y = 12$ is used in the calculation. The tapered ratio of h_b/h_0 varies from 0.0 to 2.0, and the aspect ratios, a/b of 0.5, 1.0 and 2.0 are used. The results are compared with those obtained by Kobayashi and Sonoda (1991) using the power series method. It is found that good agreement is obtained for both uniform and tapered thickness plates. The high-order strip model combined with the exact integration scheme is also efficient for the analysis of both thin and thick plates.

Table 3 shows the comparison of buckling load parameters, $n^* = \sigma_x h_0 b^2/(D_0\pi^2)$ of square Mindlin plates with uniform thickness subjected to the uniform compressive load, σ_x. The ratios of b/h_0 vary from 5 to 1000. The effect of curvature terms appearing in the expression for loss of potential energy of the applied membrane stresses on the buckling

Table 3. Comparison of buckling load parameter, $n^* = \sigma_x h_0 b^2/D_0\pi^2$, for square Mindlin plates with uniform thickness subjected to the uniform compressive load, σ_x: $b/a = 1.0$, $k-1 = 5$, $M_y = 12$, $\delta = 0.0$, $v = 0.3$ and $\zeta = 1$

Boundary conditions	b/h_0	Present method(I)	Present method(II)	3D elasticity solutions (Srinivas *et al.*, 1969)	Ritz method (Dawe *et al.*, 1982)	FSM	Thin plate solutions (Timoshenko *et al.*, 1961)
SS-SS	1000	4.000	4.000	4.000	4.000	4.000	4.000
	100	3.997	3.998	3.997			4.000
	20	3.928	3.944	3.911	3.929	3.929	4.000
	10	3.729	3.784	3.741	3.731	3.732	4.000
	20/3	3.444	—	—	3.449	3.449	4.000
	5	3.119	3.256	3.150	3.125	3.126	4.000
SS-CC	1000	7.692	7.692				7.690
	100	7.671	7.675		7.673	7.671	7.690
	20	7.228	7.299				7.690
	10	6.178	6.370		6.198	6.178	7.690
	20/3	5.040	—				7.690
	5	4.056	4.320				7.690
SS-CF	1000	1.652	1.652				
	100	1.650	1.650				
	20	1.615	1.620				
	10	1.539	1.556				
	20/3	1.438	—				
	5	1.323	1.370				

Method(I) considers the second order strain and method(II) neglects the second order strain.

load parameters is also shown. The present results are compared with those calculated by the Ritz method (Dawe *et al.*, 1982), the finite strip method (Dawe *et al.*, 1982), the three-dimensional elasticity solution (Srinivas *et al.*, 1969) and the thin plate theory (Timoshenko *et al.*, 1961). It is found that the present method(I) considering the curvature term shows good agreement with the three-dimensional elasticity solutions and with other numerical results for both thin and thick plates. The Mindlin plate theory results compare closely with the results of three-dimensional elasticity theory whilst the results of classical plate theory are in significant error for other than very thin plates.

Tables 4, 5 and 6 show the buckling load parameters, $n^* = N_y a^2/(D_0\pi^2)$ for rectangular Mindlin plates with tapered thickness in the η-direction subjected to the in-plane compressive load, N_y. The tapered thickness parameter of δ varies from 0.0 to 1.0 and the ratio

Table 4. Buckling load parameters, $n^* = N_y a^2/D_0\pi^2$, for rectangular Mindlin plates with tapered thickness in the η-direction subjected to the in-plane compressive load. N_y : $b/a = 0.5$, $k-1 = 5$, $M_r = 12$ and $\nu = 0.3$

Boundary condition	δ	b/h_0 1000	100	50	20	10	5
SS-SS	0.0	6.250	6.247	6.239	6.179	5.977	5.301
	0.25	8.775	8.770	8.754	8.649	8.295	7.156
	0.5	11.66	11.65	11.62	11.45	10.88	9.104
	0.75	14.89	14.88	14.84	14.57	13.69	11.10
	1.0	18.47 (18.47)	18.45	18.39	17.99	16.71	13.09
SS-CC	0.0	18.19	18.16	18.08	17.51	15.80	11.56
	0.25	25.47	25.42	25.27	24.29	21.42	14.86
	0.5	33.64	33.56	33.32	31.77	27.35	18.02
	0.75	42.66	42.54	42.18	39.85	33.49	20.98
	1.0	52.49 (52.49)	52.32	51.80	48.49	39.75	23.71
SS-CS	0.0	10.39	10.38	10.35	10.16	9.557	7.787
	0.25	14.89	14.88	14.83	14.50	13.44	10.53
	0.5	20.10	20.07	19.99	19.45	17.76	13.38
	0.75	25.98	25.94	25.82	24.98	22.45	16.25
	1.0	32.54	32.47	32.29	31.07	27.46	19.07
SS-CF	0.0	2.626	2.619	2.604	2.560	2.473	2.262
	0.25	4.042	4.025	3.994	3.899	3.723	3.313
	0.5	5.909	5.871	5.812	5.639	5.315	4.599
	0.75	8.297	8.225	8.125	7.830	7.283	6.123
	1.0	11.27	11.15	11.00	10.52	9.655	7.884
SS–FC	0.0	2.626	2.619	2.604	2.560	2.473	2.262
	0.25	3.457	3.449	3.432	3.376	3.261	2.959
	0.5	4.442	4.432	4.413	4.343	4.186	3.759
	0.75	5.583	5.572	5.549	5.460	5.247	4.649
	1.0	6.884	6.871	6.844	6.730	6.442	5.618
SS-SF	0.0	2.043	2.038	2.028	1.997	1.941	1.807
	0.25	3.234	3.221	3.199	3.135	3.016	2.742
	0.5	4.840	4.813	4.772	4.653	4.431	3.929
	0.75	6.918	6.869	6.801	6.599	6.220	5.377
	1.0	9.517	9.438	9.334	9.016	8.412	7.090
SS-FS	0.0	2.043	2.038	2.028	1.997	1.941	1.807
	0.25	2.631	2.625	2.613	2.577	2.506	2.325
	0.5	3.344	3.338	3.324	3.280	3.188	2.941
	0.75	4.193	4.186	4.171	4.116	3.994	3.651
	1.0	5.185	5.177	5.159	5.090	4.927	4.452
SS-FF	0.0	1.582	1.576	1.563	1.527	1.466	1.332
	0.25	2.231	2.220	2.201	2.145	2.046	1.831
	0.5	2.997	2.980	2.951	2.869	2.721	2.397
	0.75	3.890	3.864	3.825	3.709	3.496	3.031
	1.0	4.917	4.881	4.829	4.670	4.375	3.729

( ) is the result calculated by Kobayashi and Sonoda (1991).

Table 5. Buckling load parameters, $n^* = N_y a^2/D_0\pi^2$, for rectangular Mindlin plates with tapered thickness in the η-direction subjected to the in-plane compressive load, N_y: $b/a = 1.0$, $k-1 = 5$, $M_y = 12$ and $\nu = 0.3$

Boundary condition	δ	b/h_0					
		1000	100	50	20	10	5
SS-SS	0.0	4.000	3.997	3.988	3.928	3.729	3.119
	0.25	5.529	5.523	5.507	5.398	5.043	3.986
	0.5	7.110	7.101	7.074	6.891	6.305	4.657
	0.75	8.758	8.744	8.702	8.417	7.531	5.225
	1.0	10.48 (10.48)	10.46	10.40	9.987	8.736	5.723
SS-CC	0.0	6.743	6.731	6.696	6.462	5.765	4.109
	0.25	9.407	9.386	9.324	8.916	7.750	5.194
	0.5	12.32	12.28	12.18	11.54	9.750	6.112
	0.75	15.46	15.41	15.25	14.29	11.73	6.867
	1.0	18.81 (18.81)	18.73	18.52	17.15	13.65	7.479
SS-CS	0.0	4.847	4.842	4.826	4.717	4.372	3.418
	0.25	7.236	7.226	7.196	6.992	6.365	4.749
	0.5	9.990	9.973	9.920	9.570	8.522	5.945
	0.75	13.04	13.02	12.93	12.36	10.71	6.813
	1.0	16.35	16.30	16.17	15.30	12.84	7.455
SS-CF	0.0	2.392	2.378	2.351	2.260	2.078	1.666
	0.25	4.145	4.109	4.046	3.840	3.430	2.575
	0.5	6.535	6.460	6.337	5.936	5.147	3.630
	0.75	9.573	9.437	9.232	8.537	7.189	4.786
	1.0	13.19	12.98	12.67	11.58	9.486	5.992
SS-FC	0.0	2.392	2.378	2.351	2.260	2.078	1.666
	0.25	2.745	2.731	2.701	2.597	2.384	1.893
	0.5	3.130	3.114	3.081	2.964	2.713	2.129
	0.75	3.551	3.534	3.498	3.364	3.069	2.374
	1.0	4.010	3.992	3.952	3.799	3.450	2.628
SS-SF	0.0	2.366	2.353	2.326	2.237	2.060	1.657
	0.25	4.010	3.978	3.920	3.732	3.351	2.541
	0.5	6.036	5.980	5.889	5.568	4.899	3.536
	0.75	8.161	8.094	7.982	7.538	6.545	4.547
	1.0	10.19	10.12	9.998	9.439	8.104	5.404
SS-FS	0.0	2.366	2.353	2.326	2.237	2.060	1.657
	0.25	2.738	2.723	2.693	2.591	2.379	1.890
	0.5	3.129	3.113	3.080	2.963	2.713	2.129
	0.75	3.551	3.534	3.498	3.364	3.069	2.374
	1.0	4.010	3.991	3.951	3.798	3.449	2.627
SS-FF	0.0	2.043	2.032	2.011	1.942	1.807	1.497
	0.25	2.599	2.585	2.557	2.463	2.272	1.830
	0.5	3.037	3.022	2.990	2.878	2.641	2.087
	0.75	3.484	3.467	3.431	3.300	3.014	2.342
	1.0	3.958	3.939	3.899	3.747	3.405	2.600

( ) is the result calculated by Kobayashi and Sonoda (1991).

of b/h_0 changes from 5 to 1000. In the case of very thin plates, the results are compared with those calculated by Kobayashi and Sonoda (1991) using the power series method. Good agreement is obtained. The results for the thicker plates with the inclusion of transverse shear effects indicate a smaller buckling load parameter. On the other hand, the effect of the tapered thickness parameter δ, on the buckling load parameters become larger for the thinner plates.

Table 7 shows the buckling load parameters, $n^* = \sigma_x h_0 b^2/(D_0\pi^2)$ for square Mindlin plates with tapered thickness in the η-direction subjected to the uniform compressive load, σ_x. The tapered thickness parameter of δ varies from 0.0 to 1.0 and the ratio of b/h_0 changes from 5 to 1000.

Table 6. Buckling load parameters, $n^* = N_y a^2/D_0\pi^2$, for rectangular Mindlin plates with tapered thickness in the η-direction subjected to the in-plane compressive load, N_y : $b/a = 2.0$, $k-1 = 5$, $M_y = 12$ and $\nu = 0.3$

Boundary condition	δ	b/h_0 1000	100	50	20	10	5
SS-SS	0.0	4.000	3.988	3.954	3.729	3.119	1.754
	0.25	5.113	5.094	5.036	4.664	3.675	1.901
	0.5	5.954	5.927	5.847	5.342	4.063	1.977
	0.75	6.754	6.718	6.615	5.969	4.402	2.033
	1.0	7.553 (7.552)	7.508	7.378	6.577	4.711	2.076
SS-CC	0.0	4.847	4.826	4.763	4.372	3.418	1.803
	0.25	6.568	6.532	6.429	5.797	4.314	2.035
	0.5	8.165	8.111	7.961	7.050	4.997	2.127
	0.75	9.731	9.652	9.444	8.209	5.557	2.168
	1.0	11.31 (11.29)	11.20	10.92	9.311	6.039	2.186
SS-CS	0.0	4.237	4.222	4.180	3.906	3.175	1.766
	0.25	6.273	6.244	6.158	5.621	4.293	2.035
	0.5	8.031	7.981	7.840	6.984	4.992	2.127
	0.75	9.657	9.581	9.380	8.177	5.555	2.168
	1.0	11.26	11.15	10.88	9.293	6.038	2.186
SS-CF	0.0	2.310	2.283	2.226	2.022	1.637	0.9932
	0.25	4.188	4.116	3.982	3.516	2.671	1.452
	0.5	6.818	6.669	6.409	5.497	3.927	1.941
	0.75	9.653	9.566	9.324	7.898	5.343	2.168
	1.0	11.25	11.16	10.88	9.989	6.033	2.186
SS–FC	0.0	2.310	2.283	2.226	2.022	1.637	0.9925
	0.25	2.508	2.478	2.415	2.189	1.758	1.048
	0.5	2.704	2.672	2.605	2.356	1.878	1.102
	0.75	2.903	2.869	2.797	2.525	1.999	1.155
	1.0	3.108	3.072	2.995	2.699	2.121	1.207
SS-SF	0.0	2.310	2.282	2.225	2.022	1.637	0.9925
	0.25	4.187	4.116	3.982	3.516	2.671	1.452
	0.5	5.954	5.926	5.844	5.316	3.915	1.941
	0.75	6.751	6.716	6.613	5.968	4.401	2.033
	1.0	7.550	7.505	7.375	6.575	4.711	2.076
SS-FS	0.0	2.310	2.282	2.225	2.022	1.637	0.9925
	0.25	2.507	2.477	2.415	2.189	1.758	1.048
	0.5	2.703	2.671	2.604	2.355	1.878	1.102
	0.75	2.903	2.869	2.796	2.525	1.999	1.155
	1.0	3.108	3.072	2.994	2.698	2.121	1.207
SS-FF	0.0	2.260	2.234	2.180	1.987	1.618	0.9886
	0.25	2.507	2.477	2.414	2.188	1.758	1.048
	0.5	2.703	2.671	2.604	2.355	1.878	1.102
	0.75	2.903	2.869	2.796	2.525	1.999	1.155
	1.0	3.107	3.072	2.994	2.698	2.121	1.207

( ) is the result calculated by Kobayashi and Sonoda (1990).

It is seen that the results are dependent on these parameters, and the effects of δ and b/h_0 are similar to those observed in the previous set of problems.

Table 8 shows the effect of the distribution of the compressive load, σ_x, on the buckling load parameters, $n^* = \sigma_x h_0 b^2/(D_0\pi^2)$ of square Mindlin plates with both uniform thickness ($\delta = 0$) and tapered thickness ($\delta = 1.0$). Three types of compressive loads which are expressed by $\zeta = 1.0$, 0.0 and -1.0 (see Fig. 1) are used. It is found from these tables that the buckling parameters of the plates are dependent on the thickness ratio, b/h_0, and tapered ratio, δ. The buckling load parameters are also influenced by the distributing parameter, ζ, of the compressive load. The case of $\zeta = 1.0$ is the most critical one.

Figures 2 and 3 show the buckling load parameters, $n^* = \sigma_x h_0 b^2/(D_0\pi^2)$, versus the plate-aspect ratios of rectangular plates with uniform thickness and tapered thickness,

Table 7. Buckling load parameters, $n^* = \sigma_x h_0 b^2 / D_0 \pi^2$, for square Mindlin plates with tapered thickness in the η-direction subjected to the uniform compressive load, σ_x: $b/a = 1.0$, $\nu = 0.3$, $k-1 = 5$, $M_y = 12$ and $\zeta = 1$

Boundary condition	δ	b/h_0 = 1000	100	50	20	10	5
SS-SS	0.0	4.000	3.997	3.988	3.928	3.729	3.119
	0.25	5.048	5.043	5.029	4.934	4.624	3.727
	0.5	6.191	6.184	6.163	6.019	5.564	4.320
	0.75	7.428	7.418	7.387	7.181	6.542	4.893
	1.0	8.758	8.744	8.701	8.415	7.549	5.442
SS-CC	0.0	7.691	7.671	7.612	7.228	6.178	4.056
	0.25	9.671	9.640	9.547	8.955	7.416	4.594
	0.5	11.77	11.72	11.58	10.73	8.620	5.069
	0.75	13.97	13.91	13.72	12.55	9.789	5.493
	1.0	16.29	16.20	15.95	14.40	10.92	5.871
SS-CS	0.0	5.740	5.733	5.713	5.574	5.140	3.876
	0.25	7.166	7.155	7.123	6.911	6.261	4.437
	0.5	8.695	8.680	8.633	8.325	7.406	4.932
	0.75	10.33	10.31	10.24	9.811	8.567	5.372
	1.0	12.06	12.03	11.94	11.37	9.736	5.765
SS-CF	0.0	1.653	1.650	1.644	1.615	1.539	1.323
	0.25	2.178	2.173	2.163	2.116	1.989	1.642
	0.5	2.775	2.768	2.752	2.679	2.481	1.967
	0.75	3.442	3.431	3.409	3.302	3.010	2.290
	1.0	4.176	4.161	4.131	3.978	3.567	2.605
SS−FC	0.0	1.653	1.650	1.644	1.615	1.539	1.323
	0.25	2.011	2.007	1.999	1.960	1.854	1.561
	0.5	2.412	2.407	2.396	2.344	2.201	1.815
	0.75	2.859	2.853	2.839	2.770	2.580	2.082
	1.0	3.354	3.347	3.330	3.239	2.992	2.362
SS-SF	0.0	1.402	1.400	1.396	1.378	1.327	1.173
	0.25	1.861	1.858	1.851	1.821	1.734	1.478
	0.5	2.386	2.381	2.371	2.322	2.184	1.793
	0.75	2.973	2.967	2.952	2.880	2.671	2.109
	1.0	3.623	3.614	3.594	3.489	3.189	2.422
SS-FS	0.0	1.402	1.400	1.396	1.378	1.327	1.173
	0.25	1.693	1.691	1.685	1.661	1.591	1.383
	0.5	2.019	2.016	2.009	1.976	1.883	1.609
	0.75	2.381	2.378	2.369	2.326	2.203	1.848
	1.0	2.783	2.778	2.768	2.712	2.552	2.099
SS-FF	0.0	0.9523	0.9516	0.9500	0.9412	0.9146	0.8274
	0.25	1.203	1.202	1.200	1.186	1.145	1.014
	0.5	1.480	1.479	1.475	1.456	1.396	1.209
	0.75	1.785	1.784	1.779	1.751	1.667	1.412
	1.0	2.120	2.118	2.112	2.074	1.960	1.622

respectively, and are presented graphically for the ratios of $b/h_0 = 1000$ and 10. Three combinations of the boundary conditions at the unloaded edges are considered. It is found that the values of the buckling load increase with an increase in the tapered ratio, and the buckling load parameter reduces with an increase in the thickness.

4. CONCLUSIONS

This paper presents an application of the spline strip method to predict the elastic buckling load of rectangular Mindlin plates with tapered thickness in which account is taken of the effects of both transverse shear and second strain term. The effects of aspect ratios, thickness ratios and tapered ratios on the buckling load parameters of rectangular Mindlin plates subjected to some compressive loads are investigated. The main conclusions of the present work can be summarized as follows:

Table 8. The effect of non-uniformity of compressive load on buckling load parameters, $n^* = \sigma_x h_0 b^2/D_0\pi^2$, of square Mindlin plates with tapered thickness in the η-direction: $b/a = 1.0$, $\nu = 0.3$

(a) $\zeta = 1.0$

		b/h_0					
B.C.	δ	1000	100	50	20	10	5
SS-SS	1.0	8.758	8.744	8.701	8.415	7.549	5.442
	0.0	4.000	3.997	3.988	3.928	3.729	3.119
SS-CC	1.0	16.29	16.20	15.95	14.40	10.92	5.871
	0.0	7.691	7.671	7.612	7.228	6.178	4.056
SS-CS	1.0	12.06	12.03	11.94	11.37	9.736	5.765
	0.0	5.740	5.733	5.713	5.574	5.140	3.876
SS-CF	1.0	4.176	4.161	4.131	3.978	3.567	2.605
	0.0	1.653	1.650	1.644	1.615	1.539	1.323
SS-FC	1.0	3.354	3.347	3.330	3.239	2.992	2.362
	0.0	1.653	1.650	1.644	1.615	1.539	1.323
SS-SF	1.0	3.623	3.614	3.594	3.489	3.189	2.422
	0.0	1.402	1.400	1.396	1.378	1.327	1.173
SS-FS	1.0	2.783	2.778	2.768	2.712	2.552	2.099
	0.0	1.402	1.400	1.396	1.378	1.327	1.173
SS-FF	1.0	2.120	2.118	2.112	2.074	1.960	1.622
	0.0	0.9523	0.9516	0.9500	0.9412	0.9146	0.8274

(b) $\zeta = -1.0$

SS-SS	1.0	40.33	40.16	39.68	36.63	28.98	14.47
	0.0	25.53	25.46	25.26	23.96	20.34	12.57
SS-CC	1.0	61.00	60.59	59.38	52.27	34.48	15.19
	0.0	39.67	39.49	38.96	35.66	27.15	13.45
SS-CS	1.0	60.97	60.56	59.35	52.24	34.48	15.19
	0.0	39.67	39.49	38.95	35.66	27.15	13.45
SS-CF	1.0	60.96	60.54	59.34	52.23	34.48	15.19
	0.0	39.66	39.48	38.94	35.65	27.15	13.45
SS-FC	1.0	5.386	5.374	5.346	5.218	4.880	3.990
	0.0	2.791	2.785	2.771	2.718	2.589	2.238
SS-SF	1.0	40.32	40.16	39.67	36.62	28.97	14.47
	0.0	25.52	25.46	25.26	23.96	20.34	12.57
SS-FS	1.0	4.954	4.944	4.922	4.821	4.553	3.802
	0.0	2.631	2.625	2.613	2.567	2.456	2.146
SS-FF	1.0	4.889	4.876	4.850	4.741	4.466	3.722
	0.0	2.607	2.601	2.589	2.542	2.430	2.121

(1) High-order spline strip models based on the Mindlin plate theory show the high efficiency of the rapid convergence and high accuracy of buckling loads for both thin and thick plates.

(2) The buckling load parameters and buckled mode shapes of the rectangular Mindlin plates with the tapered thickness are dependent on the thickness ratios, b/h_0, tapered ratios, δ, aspect ratios, b/a, and boundary conditions.

(3) The values of buckling load parameters increase with an increase in the tapered ratio, and the buckling load reduces with an increase in the thickness.

Table 8. *Continued.*

(c) $\zeta = 0.0$

B.C.	δ	b/h_0 1000	100	50	20	10	5
SS-SS	1.0	16.09	16.07	15.99	15.49	13.95	9.317
	0.0	7.812	7.806	7.788	7.666	7.262	6.035
SS-CC	1.0	27.87	27.72	27.29	24.67	18.71	10.02
	0.0	14.71	14.67	14.55	13.77	11.65	7.467
SS-CS	1.0	24.55	24.49	24.30	23.06	18.43	9.966
	0.0	12.68	12.67	12.61	12.26	11.17	7.367
SS-CF	1.0	14.89	14.86	14.78	14.23	12.62	8.861
	0.0	6.816	6.809	6.788	6.660	6.267	5.136
SS-FC	1.0	4.167	4.158	4.137	4.032	3.748	3.014
	0.0	2.100	2.096	2.087	2.050	1.955	1.688
SS-SF	1.0	10.84	10.83	10.79	10.52	9.675	7.399
	0.0	4.771	4.768	4.759	4.703	4.522	3.939
SS-FS	1.0	3.622	3.615	3.601	3.530	3.331	2.768
	0.0	1.870	1.867	1.860	1.833	1.763	1.554
SS-FF	1.0	3.258	3.252	3.240	3.180	3.010	2.523
	0.0	1.642	1.640	1.636	1.616	1.562	1.395

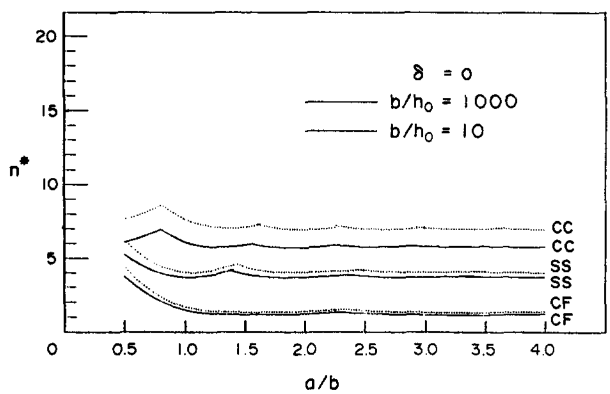

Fig. 2. Buckling coefficient, $n^* = \sigma_x h_0 b^2/D_0\pi^2$ of Mindlin plate with uniform thickness subjected to the uniform compressive load, σ_x; ($\nu = 0.3$, $\delta = 0.0$).

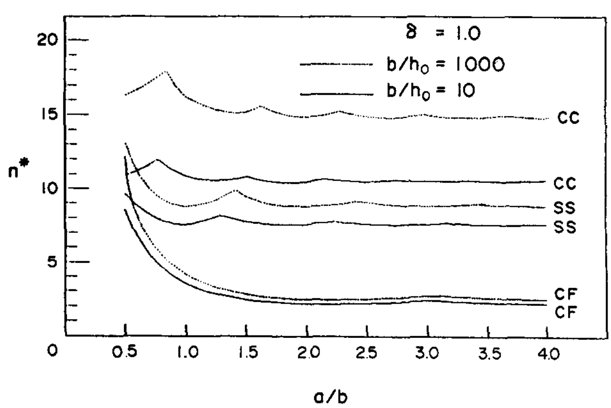

Fig. 3. Buckling coefficient, $n^* = \sigma_x h_0 b^2/D_0\pi^2$ of Mindlin plate with tapered thickness subjected to the uniform compressive load, σ_x; ($\nu = 0.3$, $\delta = 1.0$).

(4) The loading direction of compressive loads and the increment of boundary restraint are also the factors of the decrease in the buckling load parameters of the plates. In particular, the engineer's conventional intuition as to the effects of boundary restraint in raising buckling loads must be carefully modified when dealing with transversely isotropic plates.

REFERENCES

Benson, P. R. and Hinton, E. (1976). A thick finite strip solution for static, free vibration and stability problems. *Int. J. Numer. Meth. Engng* **10,** 665–678.

Brunelle, E. J. (1971). Buckling of transversely isotropic Mindlin plates. *AIAA Jl* **9,** 1018–1022.

Brunelle, E. J. and Robertson, S. R. (1974). Initially stressed Mindlin plates. *AIAA Jl* **12,** 1036–1045.

Bulson, P. S. (1970). *The Stability of Flat Plates.* Chatto and Windus, London.

Dawe, D. J. and Roufaeil, O. L. (1982). Buckling of rectangular Mindlin plates. *Comput. Struct.* **15,** 461–471.

Hinton, E. (1978). Buckling of initially stressed Mindlin plates using a finite strip method. *Comput. Struct.* **8,** 99–105.

Kobayashi, H. and Sonoda, K. (1990). Buckling of rectangular plates with tapered thickness. *J. Struct. Engng* **116,** 1278–1289.

Kobayashi, H. and Sonoda, K. (1991). Vibration and buckling of tapered rectangular plates with two opposite edges simply supported and the other two edges elastically restrained against rotation. *J. Sound Vibr.* **146,** 323–337.

Leissa, A. (1982). Advances and trends in plate buckling research. In Research in Structural and Solid Mechanics (Edited by J. M. Housner and A. K. Noor). NASA CP-2245.

Luo, J.-W. (1982). A hybrid/mixed model finite element analysis for buckling of moderately thick plates. *Comput. Struct.* **15,** 359–364.

Mizusawa, T. (1988). Application of spline strip method to analyse vibration of open cylindrical shells. *Int. J. Numer. Meth. Engng* **26,** 663–676.

Mizusawa, T. (1989). A review on application of spline functions to structural analysis. *Bull. Daido Inst. Tech.* **25,** 199–212.

Rao, G. V., Venkataramana, J. and Kanaka Raju, K. (1975). Stability of moderately thick rectangular plates using a high precision triangular element. *Comput. Struct.* **5,** 257–260.

Sakiyama, T. and Matsuda, H. (1987). Elastic buckling of rectangular Mindlin plate with mixed boundary conditions. *Comput. Struct.* **25,** 801–808.

Srinivas, S. and Rao, A. K. (1969). Buckling of thick rectangular plates. *AIAA Jl* **7,** 1645–1646.

Timoshenko, S. P. and Gere, J. M. (1961). *Theory of Elastic Stability* (2nd Edn). McGraw-Hill, New York.

APPENDIX

The sub-matrices in (22) and (23) are given as follows:

$$[K\theta_x\theta_x] = (b/a)\,\overset{003}{\mathrm{Inq}}\cdot A1 + 0.5(1-\nu)\,\overset{113}{\mathrm{Inq}}\cdot A2 + 6(1-\nu)\kappa(b/h_0)^2\,\overset{001}{\mathrm{Inq}}\cdot A2,$$

$$[K\theta_x\theta_y] = (b/a)\nu\,\overset{013}{\mathrm{Inq}}\cdot A3 + 0.5(1-\nu)(b/a)\,\overset{103}{\mathrm{Inq}}\cdot A4,$$

$$[K\theta_x W'] = 6(1-\nu)\kappa(b/a)(b/h_0)^2\,\overset{001}{\mathrm{Inq}}\cdot A4,$$

$$[K\theta_y\theta_x] = (b/a)\nu\,\overset{103}{\mathrm{Inq}}\cdot A5 + 0.5(1-\nu)(b/a)\,\overset{013}{\mathrm{Inq}}\cdot A6,$$

$$[K\theta_y\theta_y] = \overset{113}{\mathrm{Inq}}\cdot A7 + 0.5(1-\nu)(b/a)^2\,\overset{003}{\mathrm{Inq}}\cdot A8 + 6(1-\nu)\kappa(b/h_0)^2\,\overset{001}{\mathrm{Inq}}\cdot A7,$$

$$[K\theta_y W'] = 6(1-\nu)\kappa(b/h_0)^2\,\overset{011}{\mathrm{Inq}}\cdot A7,$$

$$[KW'\theta_x] = 6(1-\nu)\kappa(b/a)(b/h_0)^2\,\overset{001}{\mathrm{Inq}}\cdot A6,$$

$$[KW'\theta_y] = 6(1-\nu)\kappa(b/h_0)^2\,\overset{101}{\mathrm{Inq}}\cdot A7,$$

$$[KW'W'] = 6(1-\nu)\kappa(b/a)^2(b/h_0)^2\,\overset{001}{\mathrm{Inq}}\cdot A8 + 6(1-\nu)\kappa(b/h_0)^2\,\overset{111}{\mathrm{Inq}}\cdot A7,$$

and

$$[G\theta_x\theta_x] = (1/12)(h_0/b)^2\{N_y\,\overset{112}{\mathrm{Inq}}\cdot A2 + (b/a)^2 N_x^0\,\overset{003}{\mathrm{Inq}}\cdot A2\},$$

$$[G\theta_y\theta_y] = (1/12)(h_0/b)^2\{N_y\,\overset{112}{\mathrm{Inq}}\cdot A7 + (b/a)^2 N_x^0\,\overset{003}{\mathrm{Inq}}\cdot A7\},$$

$$[GW'W'] = \{N_y\,\overset{110}{\mathrm{Inq}}\cdot A7 + (b/a)^2 N_x^0\,\overset{001}{\mathrm{Inq}}\cdot A7\}, \qquad \text{(A1)}$$

in which the integrals Inq and Ai are given by

$$\overset{stu}{\mathrm{Inq}} = \int_0^1 \{\partial^{(s)}[\mathbf{N}]_n/\partial\eta^s \cdot \partial^{(t)}[\mathbf{N}]_q/\partial\eta^t\} \cdot (\delta\eta + 1)^u \, d\eta, \tag{A2}$$

where s and t are the order of derivatives of [N], and

$$A1 = \int_0^1 (\partial \bar{Y}m(\xi)/\partial\xi) \cdot (\partial \bar{Y}s(\xi)/\partial\xi) \, d\xi,$$

$$A2 = \int_0^1 \bar{Y}m(\xi) \cdot \bar{Y}s(\xi) \, d\xi,$$

$$A3 = \int_0^1 (\partial \bar{Y}m(\xi)/\partial\xi) \cdot Ys(\xi) \, d\xi,$$

$$A4 = \int_0^1 \bar{Y}m(\xi) \cdot (\partial Ys(\xi)/\partial\xi) \, d\xi,$$

$$A5 = \int_0^1 Ym(\xi) \cdot (\partial \bar{Y}s(\xi)/\partial\xi) \, d\xi,$$

$$A6 = \int_0^1 (\partial Ym(\xi)/\partial\xi) \cdot \bar{Y}s(\xi) \, d\xi,$$

$$A7 = \int_0^1 Ym(\xi) \cdot Ys(\xi) \, d\xi,$$

$$A8 = \int_0^1 (\partial Ym(\xi)/\partial\xi) \cdot (\partial Ys(\xi)/\partial\xi) \, d\xi.$$